CHAPTER IV
RESULTS AND DISCUSSION

4.1 Characterization of Chitin

Shrimp shells compose of three major components, which are chitin, calcium carbonate, and protein. Calcium carbonate and protein can be removed by solvent extraction and chitin will be obtained as the remaining substance.

In this research, chitin was prepared from shells of *Penaeus merguiensis* shrimp by demineralization with hydrochloric acid solution and deproteinization with sodium hydroxide solution in order to remove the calcium carbonate and the protein, respectively. The yield obtained during chitin production is shown in Table 4.1.

Table 4.1 Yield of chitin production from shrimp shell

Material	Yield* (%)
Shrimp shell	100
Product after demineralization and deproteinization (chitin)	34.17

* dry weight basis

4.1.1 Structural Characterization

FTIR spectrum of chitin is shown in Figure 4.1. The characteristic absorption bands of chitin were observed at 1648, 1554, and 1310 cm^{-1} due to the amide I, II, and III bands assigned to C=O, N-H, and C-N stretching of acetamide groups, respectively. The sharp band at 1375 cm^{-1} has been assigned to the CH_3 symmetrical deformation mode. The characteristic absorption bands of this study are similar to that of chitin reported by Sannan *et al.*, (1978).

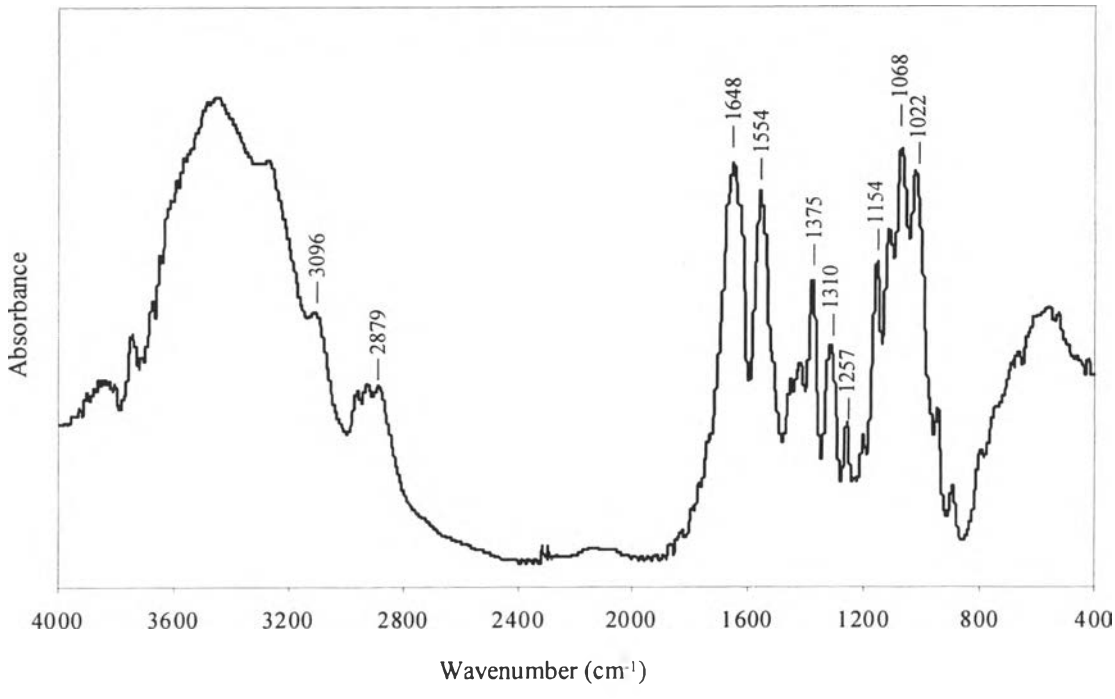

Figure 4.1 FTIR spectrum of chitin.

4.1.2 Degree of Deacetylation

Chitin has some extent of amino groups other than acetamide groups at C2 position of N-acetyl glucosamine repeating units. The degree of deacetylation of chitin depends on the nature of chitin sources and the conditions used during deproteinization. The chitin used in this study was inevitably subjected to N-deacetylation during deproteinization process under alkaline condition and heating. The degree of deacetylation of chitin determined, based on an infrared spectroscopic measurement, was 27.32%.

4.1.3 Viscosity-Average Molecular Weight

The molecular weight of chitin was determined by viscometric method and derived from its intrinsic viscosity according to the method of Lee *et al.*, (1974). The plot of reduced viscosity (η_{sp}/C) and inherent viscosity [($\ln \eta_{rel}$)/C] versus concentration of chitin solution is shown in Figure 4.2.

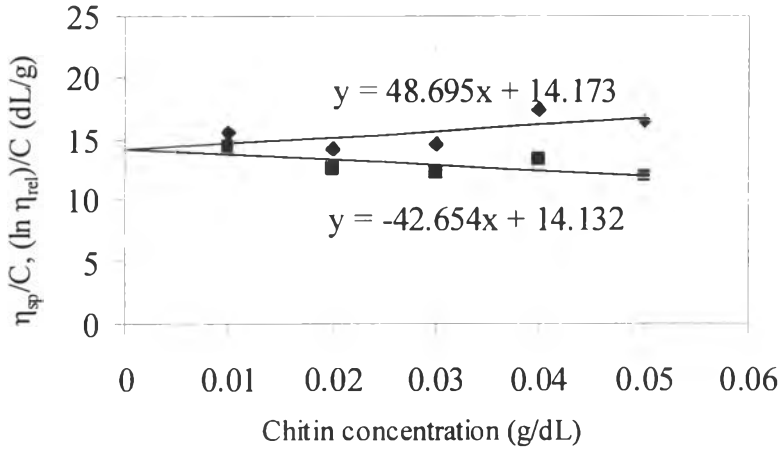

Figure 4.2 Plot of reduced viscosity (◆) and inherent viscosity (■) versus concentration of chitin solution.

From the calculation, the viscosity-average molecular weight of chitin was 824,807.

4.2 Characterization of CM-chitin

Chitin is insoluble in common solvents. However, the dissolubility of chitin can be improved by chemical modification. Chitin was modified to be CM-chitin, a water-soluble derivative, by carboxymethylation with monochloroacetic acid. Table 4.2 shows the yield of CM-chitin produced from chitin.

Table 4.2 Yield of CM-chitin production from chitin

Material	Yield* (%)
Chitin	100
Product after carboxymethylation (CM-chitin)	95.25

* dry weight basis

4.2.1 Structural Characterization

CM-chitin obtained was characterized using FTIR. The FTIR spectrum of CM-chitin is shown in Figure 4.3. The characteristic absorption peaks of CM-chitin were observed at 1732 cm^{-1} (C=O stretching of carboxylic group), 1659 cm^{-1} (C=O stretching of acetamide group), 1564 cm^{-1} (NH deformation), and 1075 cm^{-1} (C-O stretching vibration). The characteristic absorption peaks of this study are similar to that of CM-chitin reported by Muzzarelli (1988).

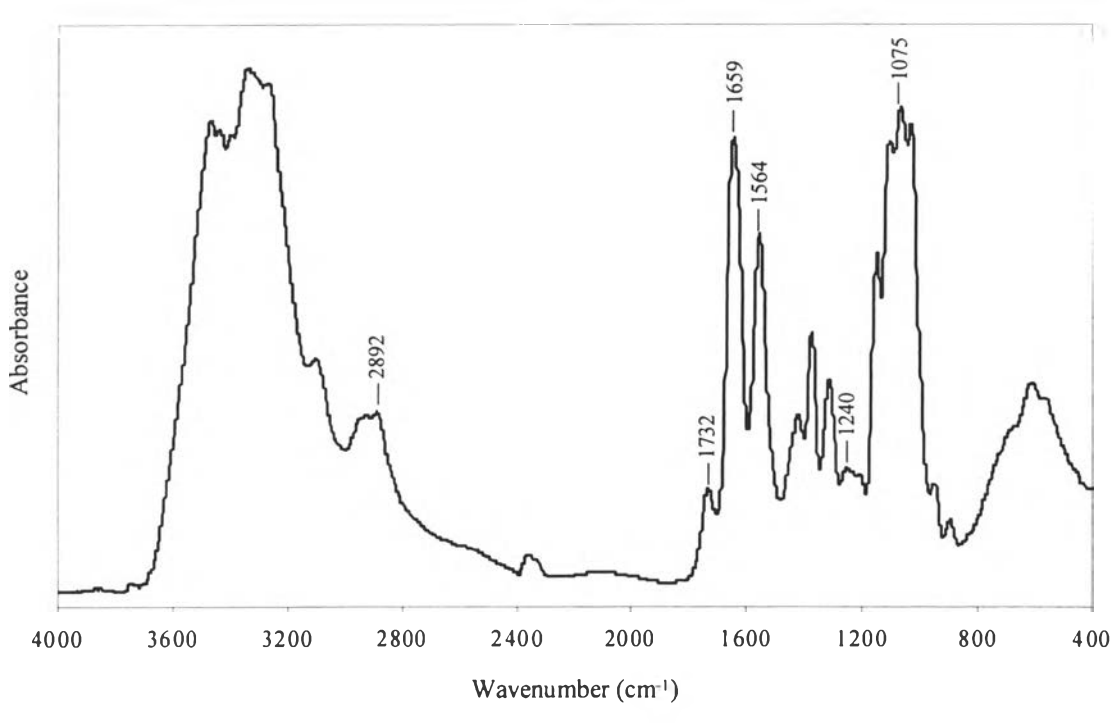

Figure 4.3 FTIR spectrum of CM-chitin.

4.2.2 Degree of Substitution

Degree of substitution of CM-chitin estimated by elemental analysis was 0.58.

4.2.3 Viscosity-Average Molecular Weight

The molecular weight of CM-chitin was determined using the intrinsic viscosity method. Figure 4.4 shows the plot between the

concentrations of the sample solution and the values of both reduced and inherent viscosities.

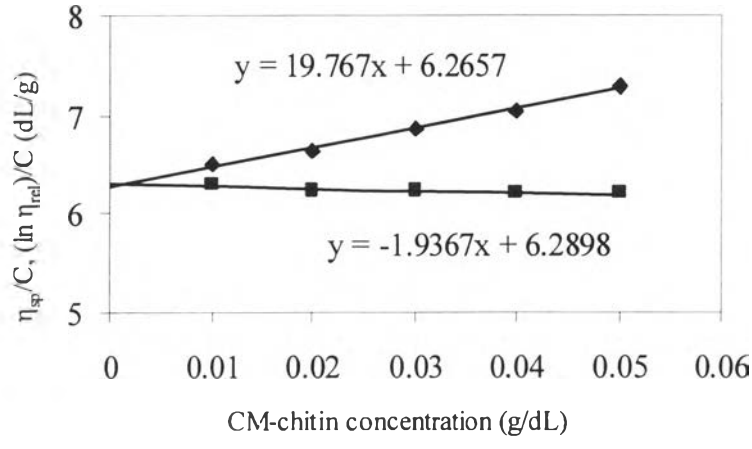

Figure 4.4 Values of reduced viscosity (◆) and inherent viscosity (■) of CM-chitin plotted against concentration.

The value of intrinsic viscosity obtained from the intercept of the plot was 6.29 dL/g. The molecular weight of CM-chitin calculated according to the method of Kaneko (1982) was 79,419.

4.3 Characterization of CM-chitosan

CM-chitosan was prepared by deacetylation of CM-chitin in alkaline and heat condition. Table 4.3 shows the yield of CM-chitosan produced from CM-chitin.

Table 4.3 Yield of CM-chitosan production from CM-chitin

Material	Yield* (%)
CM-chitin	100
Product after deacetylation (CM-chitosan)	92.86

* dry weight basis

4.3.1 Structural Characterization

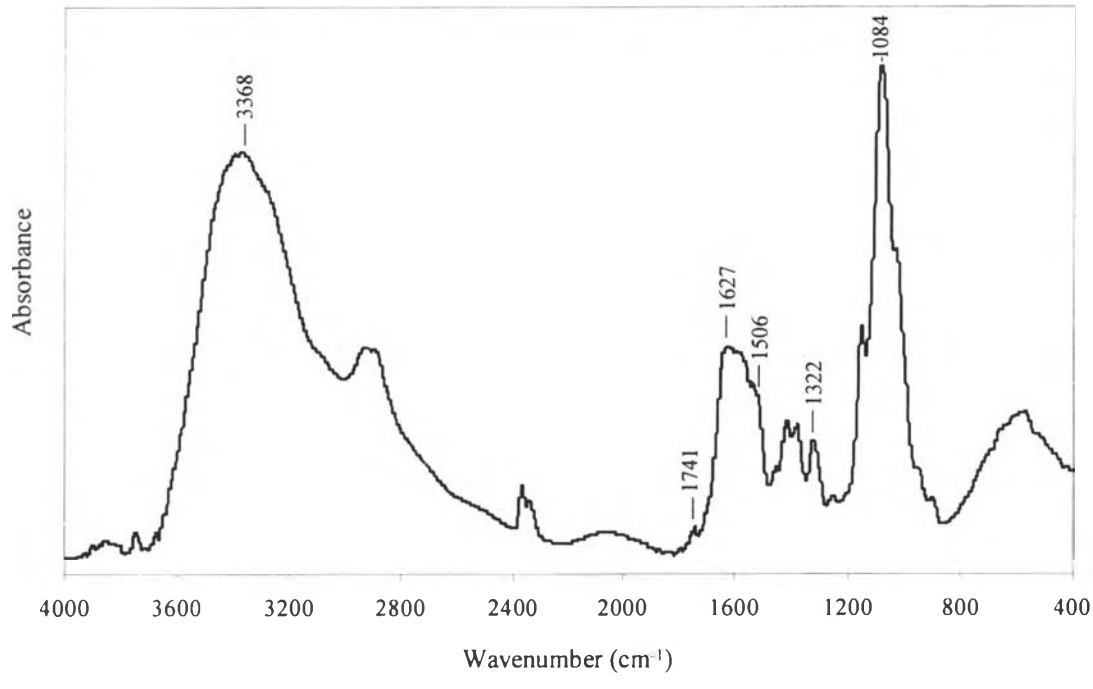

Figure 4.5 FTIR spectrum of CM-chitosan.

Figure 4.5 shows FTIR spectrum of CM-chitosan. The absorption frequencies of characteristic bands of CM-chitosan were observed at 1741 cm^{-1} (-COOH), 1084 cm^{-1} (-C-O-), and 1627 and 1506 cm^{-1} ($-NH_3^+$). The similar characteristic bands of O-CM-chitosan were also observed by Liu *et al.*, (2001).

^{13}C-NMR was used to confirm the chemical structure of CM-chitosan. ^{13}C-NMR spectrum of CM-chitosan in DSS, as shown in Figure 4.6, shows signals at 180.50 (C=O(-O)), 163.67 (C=O(-N)), 105.26 (C1), 80.81 (C4), 77.56 (C5), 76.61 (C3), 62.89 (C6), and 59.18 (C2). The resonance at 73 ppm to be the $-CH_2-$ groups both from C-3 and C-6 (Hjerde *et al.*, 1997). Moreover, the spectrum indicates the presence of $-N-CH_2-COO^-$ at 57.07 ppm (Chen *et al.*, 2002). From FTIR and ^{13}C-NMR spectra, we can deduce that the carboxymethylation of chitosan is on –OH (C3 and C6) and $-NH_2$ and N,O-(3,6)-CM-chitosan was obtained.

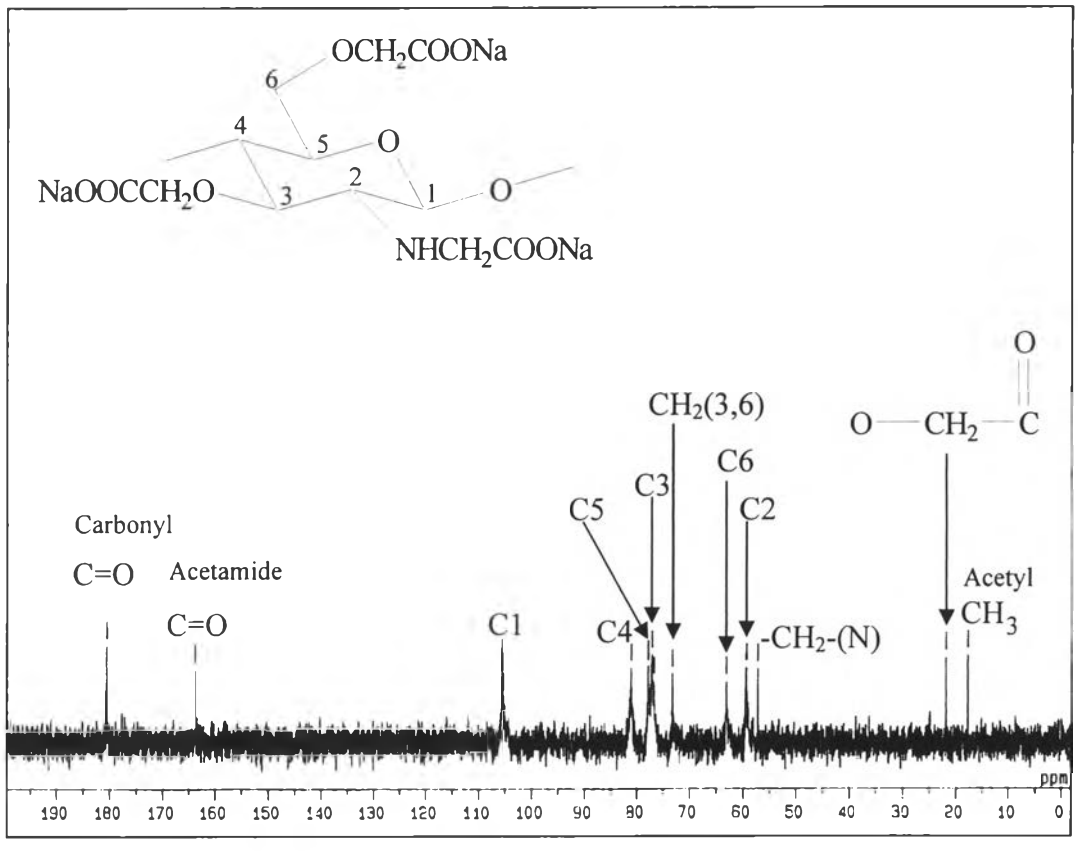

Figure 4.6 ^{13}C-NMR spectrum of CM-chitosan.

4.3.2 Degree of Substitution

The degree of substitution of CM-chitosan was confirmed by elemental analysis. The value obtained was 0.76.

4.3.3 Viscosity-Average Molecular Weight

The molecular weight of CM-chitosan was determined by viscometric method. The molecular weight of CM-chitosan was derived from its intrinsic viscosity according to the method of Kaneko (1982). The intrinsic viscosity was 3.18 dL/g. The viscosity-average molecular weight of CM-chitosan obtained from the calculation was 40,152.

Figure 4.7 shows the plot of reduced viscosity and inherent viscosity versus concentration of CM-chitosan solution.

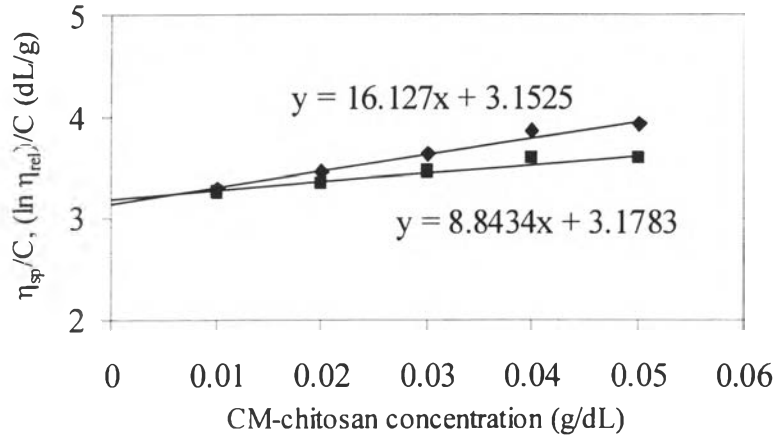

Figure 4.7 Plot of reduced viscosity (◆) and inherent viscosity (■) versus concentration of CM-chitosan solution.

4.4 Characterization of Sodium Alginate

The molecular weight of sodium alginate was determined using the intrinsic viscosity method according to the method of Yan *et al.*, (2000). Figure 4.8 shows the plot between the concentration of the sodium alginate solution and the values of both reduced and inherent viscosities.

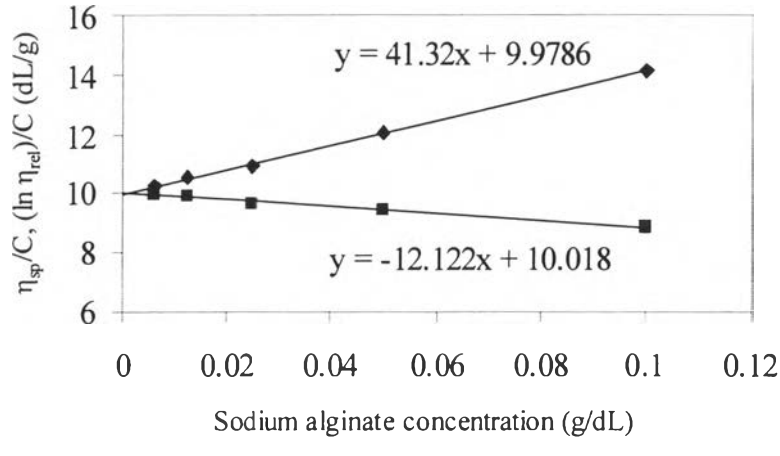

Figure 4.8 Values of reduced viscosity (◆) and inherent viscosity (■) of sodium alginate plotted against concentration.

The value of intrinsic viscosity obtained from the intercept of the plot was 10.02 dL/g. The molecular weight of sodium alginate was calculated to be 283,866.

4.5 Preparation and Characterization of CM-chitosan/alginate Blend Solution

4.5.1 Preparation of CM-chitosan/alginate Blend Solution

Three spinning solutions were prepared in this study. Pure alginate solution was a clear yellowish solution whereas 0.5% and 1.0% CM-chitosan/alginate blend solutions were turbid yellowish solutions.

4.5.2 Interaction in CM-chitosan/alginate Blend Solution

About 5 g of spinning solution and 1.0% CM-chitosan solution were prepared into film form. Weights of the films obtained from 0.5% and 1.0% CM-chitosan/alginate blend solutions were 0.331 and 0.352 g, respectively. From the calculation, the films obtained from 0.5% and 1.0% CM-chitosan/alginate blend solutions were 7.55% and 14.20% blend films, respectively. The FTIR spectra of alginate, CM-chitosan and CM-chitosan/alginate blend films with 7.55 and 14.20% CM-chitosan contents are shown in Figure 4.9. The FTIR spectrum of pure alginate shows the characteristic absorption bands at 3382, 1609, and 1036 cm^{-1} which are assigned to —OH stretching, C=O stretching, and C-O-C stretching, respectively. For pure CM-chitosan, the characteristic absorption bands were observed at 1741 cm^{-1} (C=O), 1084 cm^{-1} (C-O), and 1627 and 1506 cm^{-1} (—NH_3^+). In the blends, the —OH stretching vibration bands (at 3300 and 3280 cm^{-1}) were broadened and shifted to lower wavenumber compared to pure alginate and pure CM-chitosan, suggesting that intermolecular hydrogen bonds involving hydroxyl groups exist in the polymer chains. Furthermore, the peak became more broaden with increasing CM-chitosan content in the blend. In addition, the absorption band at 1609 cm^{-1} of pure alginate was shifted to higher wavenumber at around 1630 cm^{-1} by blending with CM-chitosan. Moreover, the intensities of the absorption bands at around 1740 cm^{-1} became

higher in the blends as compared to pure CM-chitosan. The increasing in absorption intensities at 1740 cm^{-1} in the blends might be caused by electrostatic interaction between —COOH groups of alginic acid and —NH_2 groups of CM-chitosan present in the blends (Zhang *et al.*, 2000). The FTIR results indicated that the electrostatic force and intermolecular hydrogen bonding occurred in the blend between alginate and CM-chitosan.

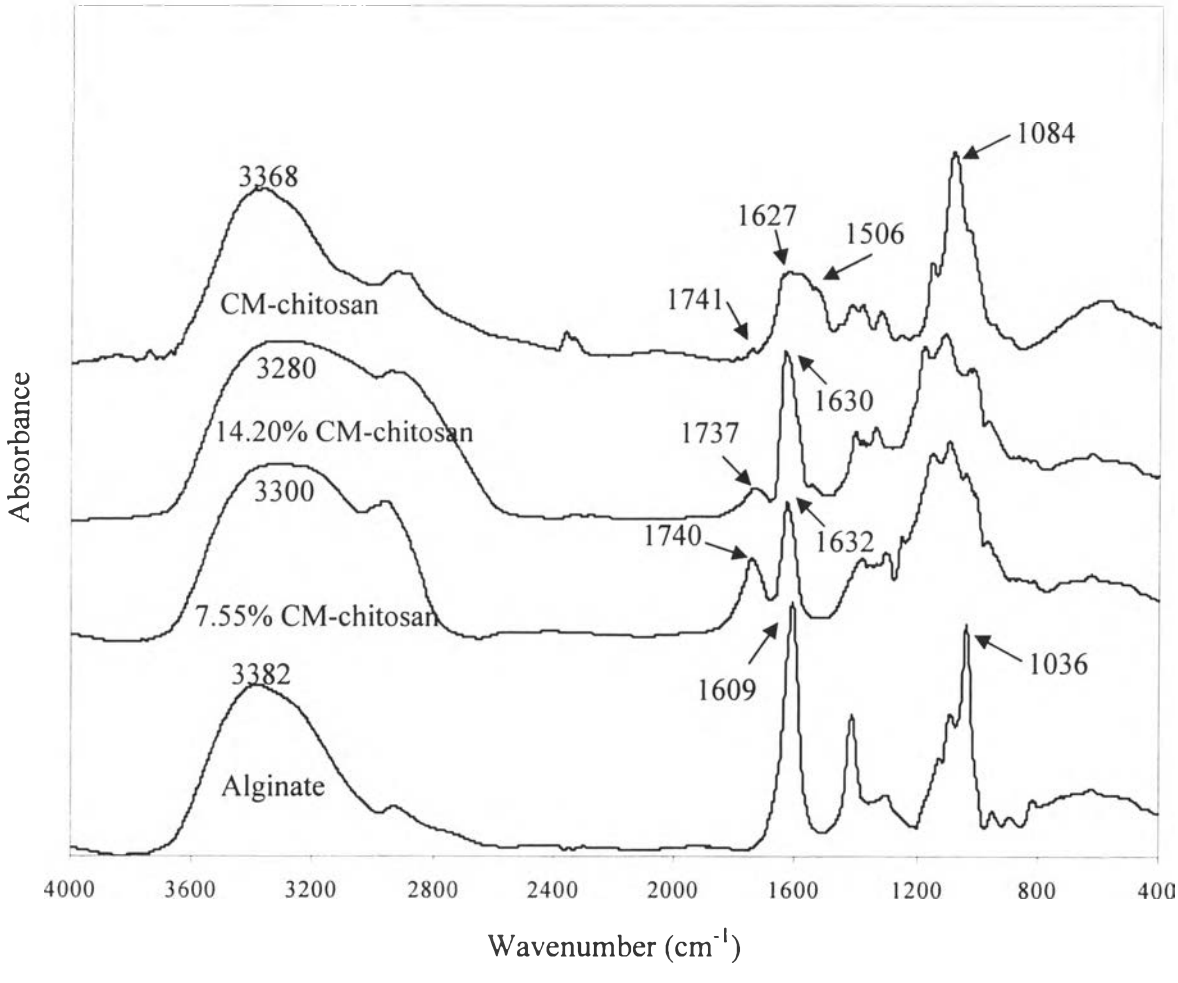

Figure 4.9 FTIR spectra of alginate, CM-chitosan and CM-chitosan/alginate blend films with 7.55 and 14.20% CM-chitosan contents.

4.6 Characterization of CM-chitosan/alginate Blend Fiber

About 195 g of spinning solutions were spun into fiber form. Weights of the fibers spun from 0.5% and 1.0% CM-chitosan/alginate blend solutions were 11.78 and 13.30 g, respectively. From the calculation, the fibers spun from 0.5% and 1.0% CM-chitosan/alginate blend solutions were 8.28% and 14.66% blend fibers, respectively.

4.6.1 SEM Micrographs of CM-chitosan/alginate Blend Fiber

In this study, SEM was used to observe fiber surface. SEM micrographs of the blend fibers are shown in Figure 4.10.

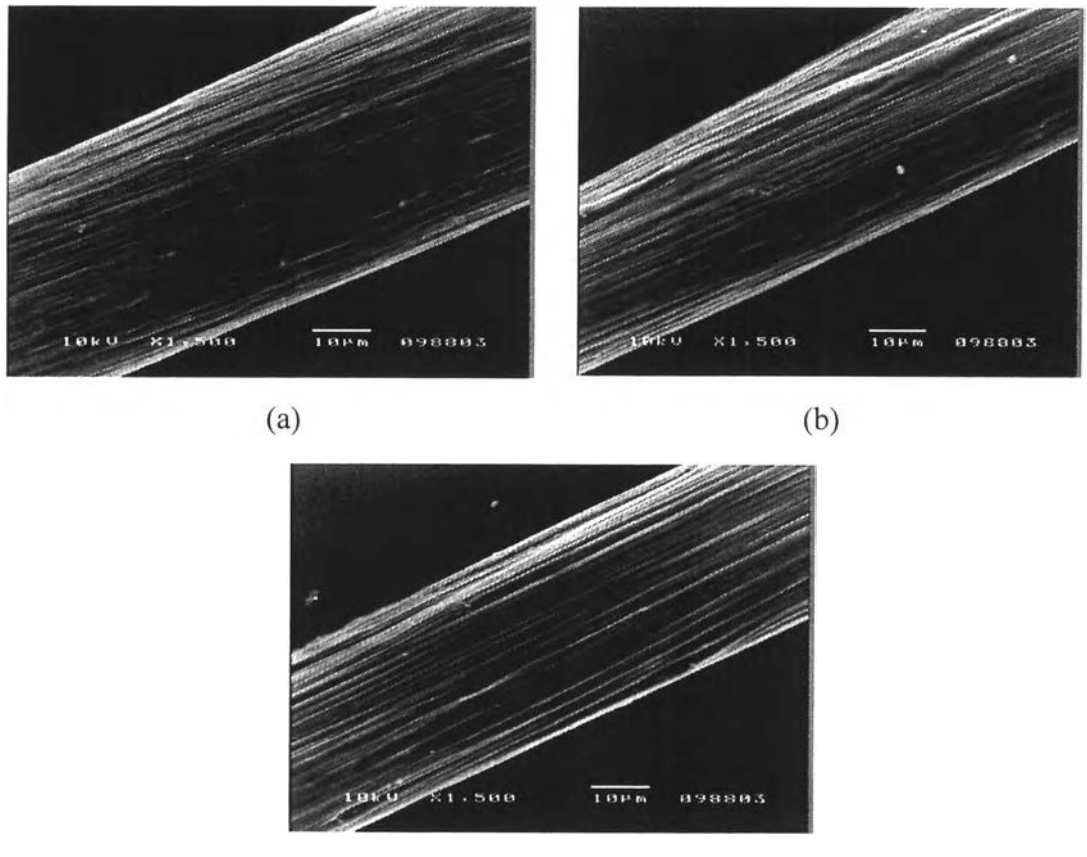

Figure 4.10 SEM micrographs of (a) alginate fiber, (b) 8.28% CM-chitosan/alginate blend fiber and (c) 14.66% CM-chitosan/alginate blend fiber.

It was found that there was no noticeable change in the surface morphology of the fibers spun with different CM-chitosan contents in the spinning dopes as studied in this work.

4.6.2 Calcium Content in CM-chitosan/alginate Blend Fiber

Table 4.4 shows the calcium contents in the pure alginate and CM-chitosan/alginate blend fibers.

Table 4.4 Calcium content in alginate and CM-chitosan/alginate blend fibers

Fiber	Calcium content (mg/100 g fiber)
Alginate fiber	8301.53
8.28% CM-chitosan/alginate blend fiber	7017.54
14.66% CM-chitosan/alginate blend fiber	6679.76

The calcium contents in the CM-chitosan/alginate blend fibers were lower than that in the pure alginate fiber. Furthermore, the calcium content in the 14.66% CM-chitosan/alginate blend fiber was lower than that in 8.28% CM-chitosan/alginate blend fiber. This may be due to the decrease in alginate content in the CM-chitosan/alginate blend fibers as the CM-chitosan content in the blend fibers increased. The lower the alginate content, the less the calcium ions trapped in the blend fibers.

4.6.3 Mechanical Properties of CM-chitosan/alginate Blend Fiber

Mechanical properties of the CM-chitosan/alginate blend fibers are summarized in Table 4.5. The tensile strengths of the blend fibers were lower than that of the pure alginate fiber and decreased with increasing of CM-chitosan content. It is known that calcium ion plays an important role in cross-linking of alginate. Therefore, the decreasing of calcium ion in blend fibers resulted in less cross-linking occurring in the blend fibers as compared to pure alginate fiber. In addition, pure CM-chitosan and pure alginate films were prepared to determine their tensile strengths. It was found that the

tensile strength of pure CM-chitosan film (59.66 MPa) was lower than that of pure alginate film (78.56 MPa). This result indicated that CM-chitosan caused the weakness in the blend fibers compared to pure alginate fiber. However, the values of elongation at break for the blend fibers were higher than that for pure alginate fiber and increased with increasing CM-chitosan contents. Moreover, the linear densities of the blend fibers were lower than that of the pure alginate fiber. This might be due to the lower calcium content in the blend fibers.

Table 4.5 Mechanical properties of alginate and CM-chitosan/alginate blend fibers

Fiber	Linear density (tex)[a]	Tensile strength (cN/tex)[a]	Elongation at break (%)[a]
Alginate fiber	51.30 ± 1.67	12.34 ± 0.24	11.69 ± 0.50
8.28% CM-chitosan/alginate blend fiber	41.44 ± 0.53	11.66 ± 0.59	13.18 ± 0.45
14.66% CM-chitosan/alginate blend fiber	37.21 ± 1.30	9.94 ± 0.37	14.02 ± 0.57

[a] Average of 20 fiber samples.

4.6.4 Antibacterial Properties of CM-chitosan/alginate Blend Fiber

Antibacterial activities of the CM-chitosan/alginate blend fibers against *E. coli* and *S. aureus* were qualitatively investigated by observing the clear zone. The clear zone was observed between the fiber and luxuriant bacteria colonies. Figure 4.11 and 4.12 show antibacterial tests of the CM-chitosan/alginate blend fibers against *E. coli* and *S. aureus*, respectively.

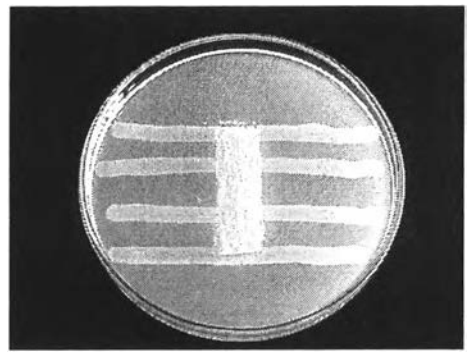

(a)

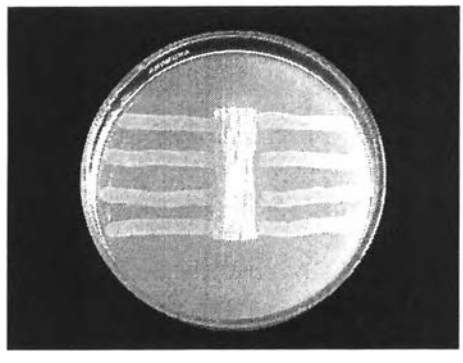

(b)

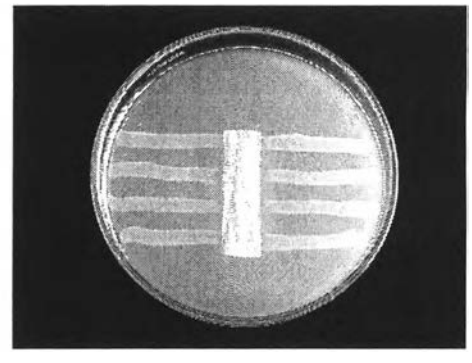

(c)

Figure 4.11 Antibacterial test against *E. coli* of (a) alginate fiber, (b) 8.28% CM-chitosan/alginate blend fiber and (c) 14.66% CM-chitosan/alginate blend fiber.

(a)

(b) (c)

Figure 4.12 Antibacterial test against *S. aureus* of (a) alginate fiber, (b) 8.28% CM-chitosan/alginate blend fiber and (c) 14.66% CM-chitosan/alginate blend fiber.

Table 4.6 shows the antibacterial test against *E. coli* and *S. aureus* of CM-chitosan/alginate blend fibers with the fiber area of about 1 cm x 4.5 cm. The CM-chitosan contents in the tested 8.28 and 14.66% CM-chitosan/alginate blend fibers were about 6.98 and 11.15 mg, respectively. The clear zone widths were observed to be varied from 0.8 to 2.0 mm. The clear zone surrounding the tested fibers was an evidence that the CM-chitosan/alginate blend fibers could inhibit the growth of *E. coli* and *S. aureus*. Moreover, Liu *et al.*, (2001) reported that CM-chitosan inhibited the growth of *E. coli* using the optical density method to investigate its antibacterial action.

It can be concluded that CM-chitosan in the CM-chitosan/alginate blend fibers acted as antibacterial agent for alginate fibers.

Table 4.6 Antibacterial test against *E. coli* and *S. aureus* of CM-chitosan/alginate blend fibers

CM-chitosan concentration (%)	Clear zone width (mm)	
	E. coli	*S. aureus*
8.28	1.0 ± 0.5	1.5 ± 0.5
14.66	0.8 ± 0.3	2.0 ± 0.5

4.7 Characterization of Chitosan-Coated Alginate Fiber

4.7.1 Confirmation of Chitosan Coating

The presence of chitosan on the chitosan-coated alginate fiber was confirmed by dissolving chitosan from the fiber using acetic acid solution. The color of the ninhydrin-tested chitosan solutions extracted from the coated alginate fibers was light yellow before heating and became dark yellow after heating whereas the color of ninhydrin-tested solution extracted from pure alginate fiber was still light yellow after heating. Generally, amino groups react with ninhydrin to give a product with blue to blue-violet color. However, Sheng *et al.*, (1993) who studied colorimetric assay of L-asparagine using ninhydrin and found that the reaction between amino groups and ninhydrin gave color change to dark yellow. The UV/Visible spectra of the extracted solutions tested with ninhydrin are shown in Figure 4.13.

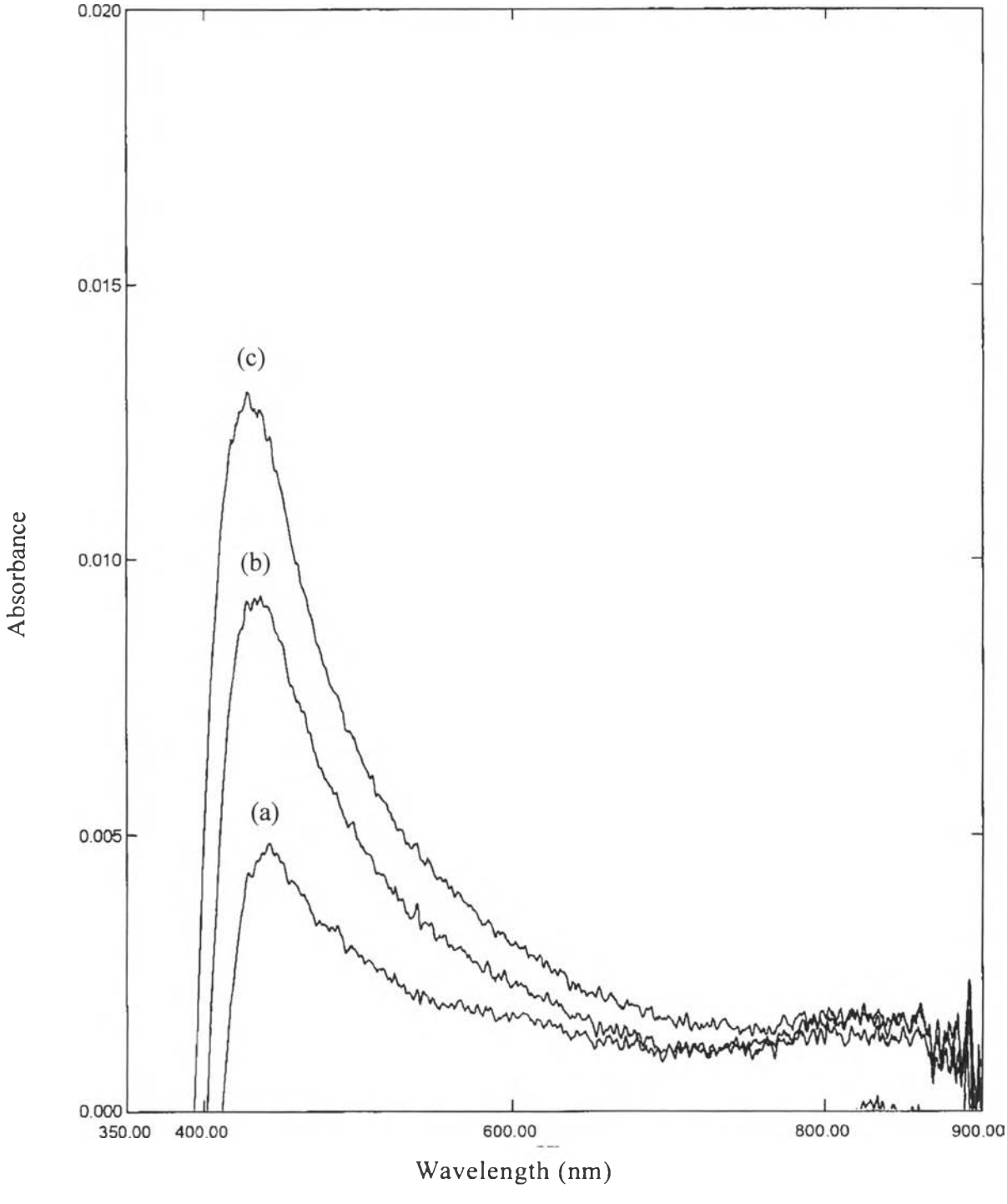

Figure 4.13 UV/Visible spectra of ninhydrin-tested chitosan solutions extracted from alginate fibers spun through the first coagulation bath containing different chitosan concentrations: (a) 2.2 x 10^{-2}%, (b) 6.7 x 10^{-2}%, and (c) 11.1 x 10^{-2}%.

The spectra show the absorption peaks at 440 nm, which is a typical value for a material containing amino groups that are treated with ninhydrin solution leading to the color change of solution to dark yellow (Sheng *et al.*, 1993). However, no peak was observed in the UV/Visible spectra of ninhydrin-tested solution extracted from pure alginate fibers. The absorbance intensities of the peaks at 440 nm increased with increasing concentration of chitosan solution in the first coagulation bath, indicating the increasing of the amounts of chitosan extracted from the chitosan-coated alginate fibers. In addition, the calculations from the absorbance intensities of the peaks and calibration curve yielded the chitosan contents coated on the alginate fibers of 21.066, 22.482, and 23.073 mg/100g fiber for the chitosan concentrations in the first coagulation bath of 2.2 x 10^{-2}%, 6.7 x 10^{-2}%, and 11.1 x 10^{-2}% w/v, respectively. The results show evidence that the alginate fibers were coated with chitosan and the chitosan contents coated on the alginate fibers increased with increasing concentration of chitosan solution in the first coagulation bath.

4.7.2 SEM Micrographs of Chitosan-Coated Alginate Fiber

Figure 4.14 shows the SEM images of the coated alginate fibers spun through the first coagulation bath containing different concentrations of chitosan solutions. Although the surface of the alginate fibers without coating was smooth, it became uneven as the concentration of chitosan in the first coagulation bath increased.

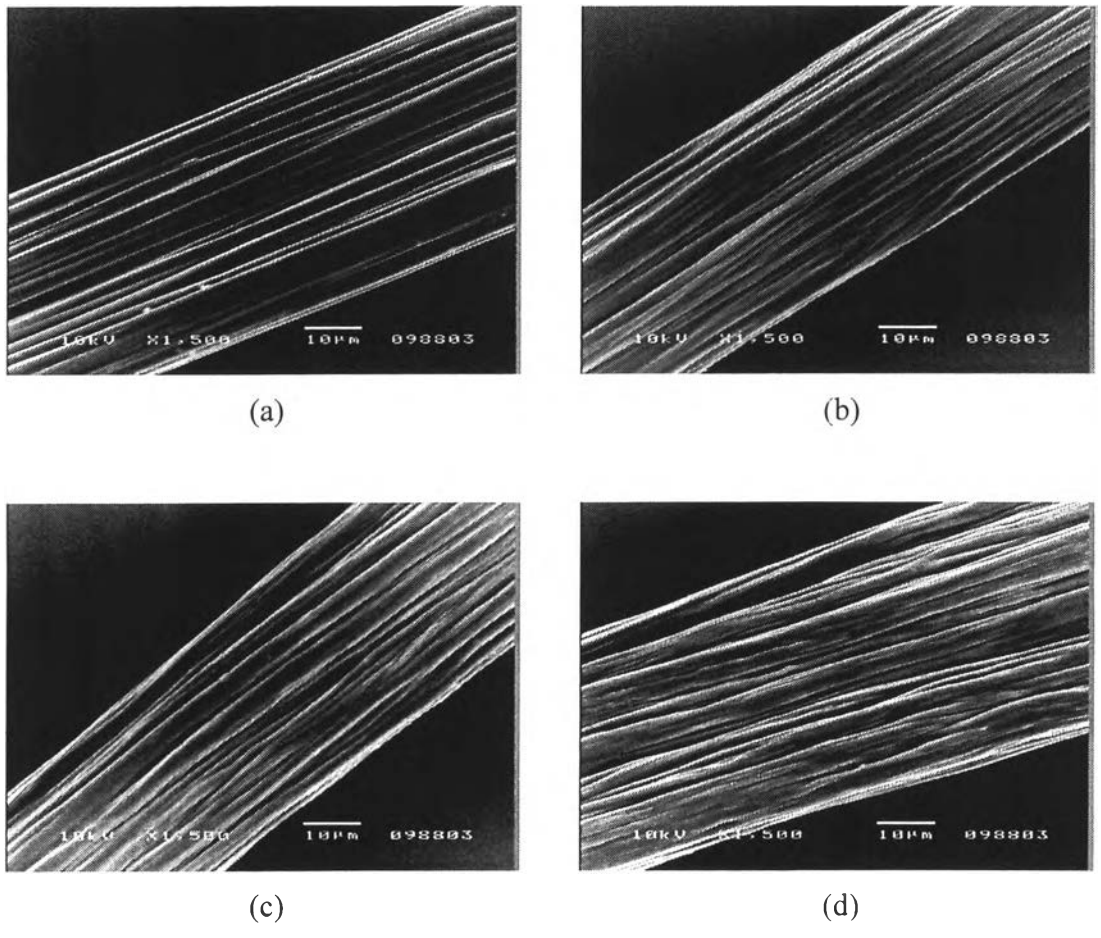

Figure 4.14 SEM micrographs of chitosan-coated alginate fibers spun through the first coagulation bath containing different chitosan concentrations: (a) 0%, (b) 2.2 x 10^{-2}%, (c) 6.7 x 10^{-2}% and (d) 11.1 x 10^{-2}%.

4.7.3 Calcium Content in Chitosan-Coated Alginate Fiber

Table 4.7 shows the calcium content in the pure alginate and chitosan-coated alginate fibers. The calcium content in the chitosan-coated alginate fibers was higher than that in the pure alginate fiber. This result might be explained by the chelating property of chitosan (Struszczyk, 1997). Chitosan acts as chelating agent because nitrogen atoms in the chitosan have lone-pair electrons which can chelate with metal ions. In this study, chitosan coated on alginate fiber could also chelate with calcium ions in the first coagulation bath resulting in the increasing of calcium content in the chitosan-coated alginate fibers as compared to that in the pure alginate fiber. However,

the calcium content in the chitosan-coated alginate fibers decreased with increasing chitosan content coated on the alginate fibers. This might be explained that the increasing of chitosan content coated on the alginate fibers resulted in the reduction of the penetration of calcium into the alginate fibers.

Table 4.7 Calcium content in alginate fibers spun through the first coagulation bath containing different chitosan concentrations

Chitosan concentration (%)	Calcium content (mg/100 g fiber)
0	8204.63
2.2×10^{-2}	9073.36
6.7×10^{-2}	8524.90
11.1×10^{-2}	8217.82

4.7.4 Mechanical Properties of Chitosan-Coated Alginate Fiber

Table 4.8 shows the mechanical properties of the chitosan-coated alginate fibers spun through the first coagulation bath containing different concentrations of chitosan solution.

Table 4.8 Mechanical properties of the alginate fibers spun through the first coagulation bath containing different chitosan concentrations

Chitosan concentration (%)	Linear density (tex)[a]	Tensile strength (cN/tex)[a]	Elongation at break (%)[a]
0	26.46 ± 1.09	10.35 ± 0.88	14.10 ± 1.92
2.2×10^{-2}	35.59 ± 0.61	12.43 ± 0.68	16.48 ± 1.49
6.7×10^{-2}	41.27 ± 1.38	12.38 ± 0.80	18.16 ± 0.65
11.1×10^{-2}	45.31 ± 1.11	12.61 ± 0.39	19.89 ± 0.69

[a] Average of 20 fiber samples.

The tensile strengths of the chitosan-coated alginate fibers were higher than that of the pure alginate fiber. It has been reported that chitosan deposits on alginate fiber due to the electrostatic interaction (Tamura *et al.*, 2002). Therefore, the presence of electrostatic interaction between chitosan and alginate in chitosan-coated alginate fibers resulted in the improvement of tensile strength of the chitosan-coated alginate fibers as compared to pure alginate fiber (Tamura *et al.*, 2002). However, there was no significant change of tensile strength of the chitosan-coated alginate fibers when the concentration of chitosan in the first coagulation bath increased. Moreover, the elongation at break for the chitosan-coated alginate fibers increased with increasing chitosan concentration in the first coagulation bath. The reason for this is that the amount of calcium ions penetrated into the alginate fibers decreased due to the increasing of chitosan coated on the surface of alginate fibers. From Table 4.8, the linear densities of the chitosan-coated alginate fibers were higher than that of pure alginate fiber and increased with increasing of chitosan concentration in the first coagulation bath. The increase in linear densities of the chitosan-coated alginate fibers suggested that the amount of chitosan coated on the surface of alginate fibers increased.

4.7.5 Antibacterial Properties of Chitosan-Coated Alginate Fiber

Antibacterial activities of the chitosan-coated alginate fibers against *E. coli* and *S. aureus* were qualitatively investigated by observing the clear zone. The clear zone was observed between the fiber and luxuriant bacteria colonies. Figure 4.15 and 4.16 show antibacterial tests of the chitosan-coated alginate fibers against *E. coli* and *S. aureus*, respectively.

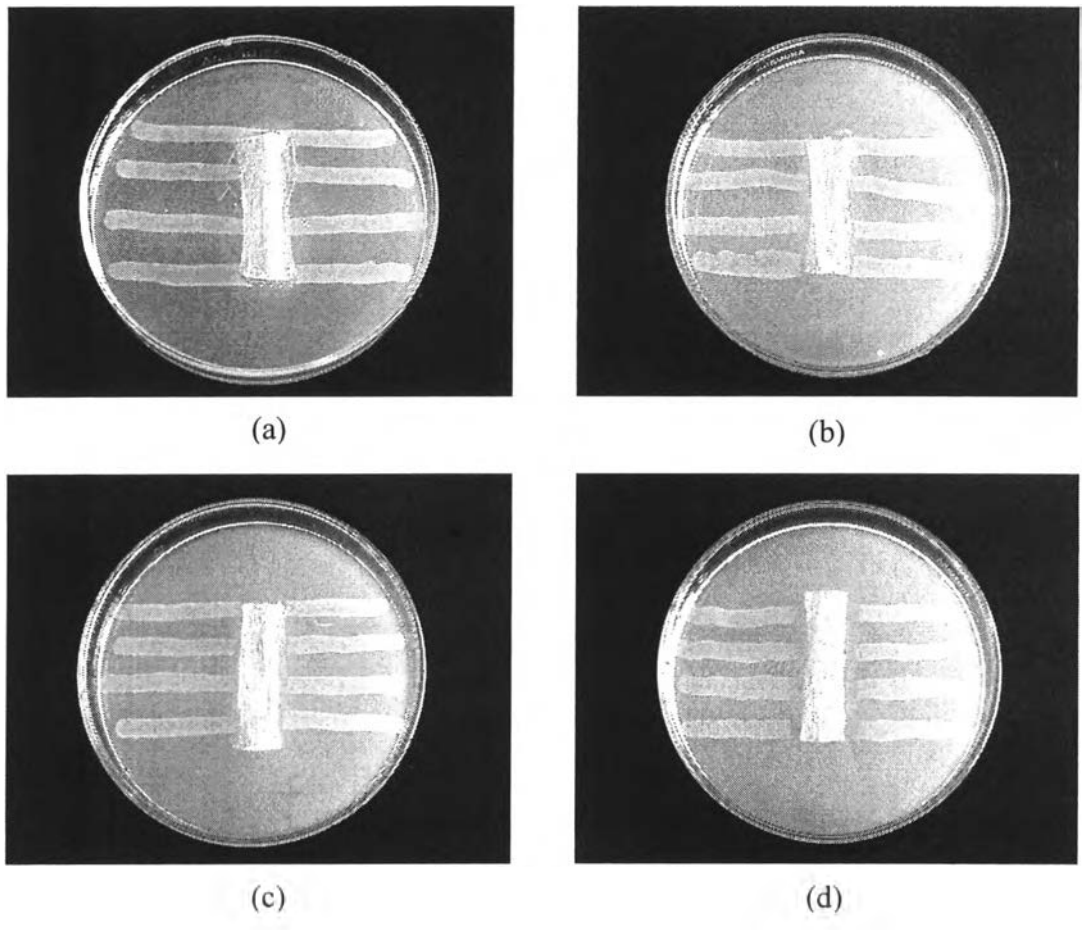

Figure 4.15 Antibacterial test against *E. coli* of chitosan-coated alginate fibers. Chitosan concentrations in the first coagulation bath (a) 0%, (b) 2.2 x 10^{-2}%, (c) 6.7 x 10^{-2}% and (d) 11.1 x 10^{-2}%.

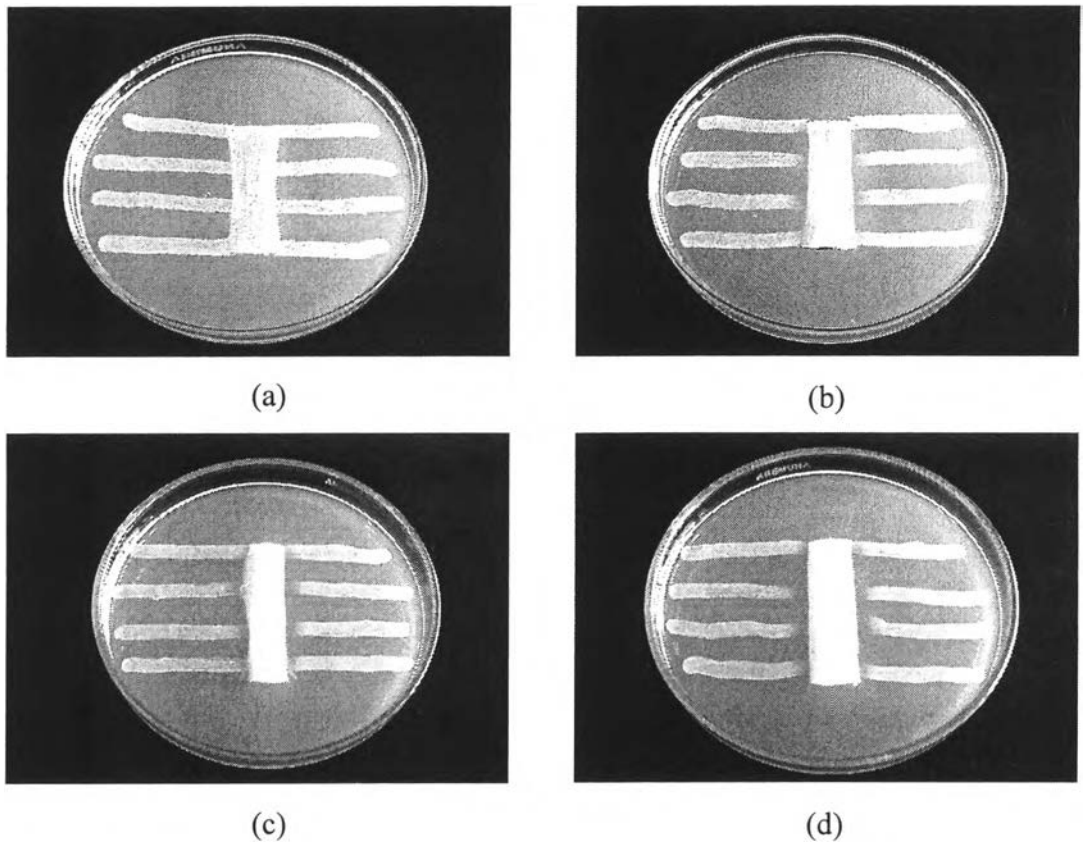

Figure 4.16 Antibacterial test against *S. aureus* of chitosan-coated alginate fibers. Chitosan concentrations in the first coagulation bath (a) 0%, (b) 2.2 x 10^{-2}%, (c) 6.7 x 10^{-2}% and (d) 11.1 x 10^{-2}%.

Table 4.9 shows the antibacterial test against *E. coli* and *S. aureus* of chitosan-coated alginate fibers with the fiber area of about 1 cm x 4.5 cm. The chitosan contents coated on the tested alginate fibers spun through the first coagulation bath containing 2.2 x 10^{-2}%, 6.7 x 10^{-2}% and 11.1 x 10^{-2}% chitosan solution were 0.016, 0.020 and 0.021 mg, respectively. The clear zone widths were observed to be varied from 0.7 to 2.2 mm. The clear zone surrounding the tested fibers was an evidence that chitosan-coated alginate fibers could inhibit the growth of *E. coli* and *S. aureus*.

Table 4.9 Antibacterial test against *E. coli* and *S. aureus* of chitosan-coated alginate fibers spun through the first coagulation bath containing different chitosan concentrations

Chitosan concentration (%)	Clear zone width (mm)	
	E. coli	*S. aureus*
2.2×10^{-2}	0.7 ± 0.3	1.0 ± 0.5
6.7×10^{-2}	1.5 ± 0.5	1.7 ± 0.3
11.1×10^{-2}	2.0 ± 0.5	2.2 ± 0.3

Higher antibacterial activity of chitosan investigated by a paper disc method was reported by No *et al.* (2002), who observed that chitosan (Mw ranging from 59,000 to 1,671,000 at 0.1% concentration) inhibited growth of many bacteria and the values of clear zone diameter were higher than 14 mm. Moreover, Liu *et al.*, (2001) reported that chitosan inhibited the growth of *E. coli* using the optical density method to investigate its antibacterial action. It can be concluded that chitosan on the chitosan-coated alginate fibers acted as antibacterial agent for alginate fibers.